

Supporting Information

A pH-sensitive nanoplatform encapsulating lipid droplets specific near-infrared fluorescent probe for *in vivo* imaging of mice carotid artery plaques

Ying Zhang^{†,a,b,c}, Tianyi Qu^{†,a,b,c}, Fengming Wu^{a,b,c}, Ming Chen^{a,b,c}, Zheng Chai^{a,b,c}, Shufen Li^{*a,c}, Weihua Zhuang^{*c,d}, and Mao Chen^{*a,b,c}

^a Laboratory of Cardiac Structure and Function, Institute of Cardiovascular Diseases, West China Hospital, Sichuan University, Chengdu, 610041, China.

^b Department of Cardiology, West China Hospital, Sichuan University, Chengdu, 610041, China.

^c Cardiac Structure and Function Research Key Laboratory of Sichuan Province, West China Hospital, Sichuan University, Chengdu, 610041, China.

^d Precision Medicine Translational Research Center, West China Hospital, Sichuan University, Chengdu 610041, China.

[†] Ying Zhang and Tianyi Qu contributed equally to this work.

* Corresponding author, Email address: chenmao@scu.edu.cn, weihuaz@scu.edu.cn and lisf20@scu.edu.cn.

Equipment and Methods

Figure S1. Synthetic route of **ZY-P1**.

Figure S2. ^1H NMR spectrum of **ZY-P1**.

Figure S3. ^{13}C NMR spectrum of **ZY-P1**.

Figure S4. Normalized absorption and emission spectrum of **ZY-P1** in PBS.

Figure S5. Emission spectra of **ZY-P1** in different solvents.

Figure S6. Relative cell viability of HeLa cells co-cultured with different concentrations of **ZY-P1** for 24 h.

Figure S7. Relative cell viability of HUVEC cells co-cultured with different concentrations of **ZY-P1** for 24 h.

Figure S8. Temporal scanning images of HeLa cells stained with **ZY-P1**.

Figure S9. Photostability of **ZY-P1**.

Figure S10. Synthetic route of **AEMA**.

Figure S11. ^1H NMR spectrum of **AEMA**.

Figure S12. Synthetic route of **PMEA**.

Figure S13. ^1H NMR spectrum of **PMPC**.

Figure S14. ^{13}C NMR spectrum of **PMPC**.

Figure S15. ^1H NMR spectrum of **PMEA**.

Figure S16. ^{13}C NMR spectrum of **PMEA**.

Figure S17. Photophysical studies of NPs.

Figure S18. TEM image of **ZY-P1-PMEA** NPs at pH 6.5.

Figure S19. Particle size variation of **ZY-P1-PMEA** NPs at different time points (pH = 4.0).

Figure S20. Zeta potential variation of **ZY-P1-PMEA** NPs at different time points (pH = 4.0).

Figure S21. Particle size variation and Zeta potential variation of **ZY-P1-PMEA** NPs at pH 8.

Figure S22. Particle size variation and Zeta potential variation of **ZY-P1-PMEA** NPs at pH 9.

Figure S23. Particle size variation and Zeta potential variation of **ZY-P1-PMEA** NPs

at pH 10.

Figure S24. Emission spectra of **ZY-P1-PMEA** NPs in PBS (pH = 4.0) at different time points.

Figure S25. Emission spectra of **ZY-P1-PMEA** NPs in PBS (pH = 6.5) at different time points.

Figure S26. Emission spectra of **ZY-P1-PMEA** NPs in PBS (pH = 8.0) at different time points.

Figure S27. Emission spectra of **ZY-P1-PMEA** NPs in PBS (pH = 9.0) at different time points.

Figure S28. Emission spectra of **ZY-P1-PMEA** NPs in PBS (pH = 10.0) at different time points.

Figure S29. Particle size variation and Zeta potential of **ZY-P1-PMEA** NPs incubation with BSA solution.

Figure S30. Relative cell viability of HeLa cells co-cultured with different concentrations of **ZY-P1-PMEA** NPs for 24 h.

Figure S31. Relative cell viability of HUVEC cells co-cultured with different concentrations of **ZY-P1-PMEA** NPs for 24 h.

Figure S32. Relative cell viability of HeLa cells co-cultured with different concentrations of **PMEA** NPs for 24 h.

Figure S33. Relative cell viability of HUVEC cells co-cultured with different concentrations of **PMEA** NPs for 24 h.

Figure S34. Cellular uptake of **ZY-P1-PMEA** NPs.

Figure S35. Colocalization imaging of HeLa cells stained with BODIPY 493/503 Green and **PMEA** NPs.

Figure S36. Colocalization imaging of HeLa cells stained with LysoTracker Green and **ZY-P1-PMEA** NPs.

Figure S37. Colocalization imaging of HeLa cells stained with MitoTracker Blue and **ZY-P1-PMEA** NPs.

Figure S38. *In vivo* fluorescence image of ApoE^{-/-} mice following tail vein injection of saline.

Figure S39. *In vivo* fluorescence image of ApoE^{-/-} mice following tail vein injection of **ZY-P1-PMEA** NPs.

Figure S40. *In vivo* fluorescence image of ApoE^{-/-} mice following tail vein injection of **ZY-P1**.

Figure S41. Pharmacokinetic analysis.

Figure S42. Oil Red O staining of aortic sections from ApoE^{-/-} mice.

Figure S43. H&E staining of major organs sections from ApoE^{-/-} mice treated with saline or **ZY-P1-PMEA** NPs.

Figure S44. Quantitative analysis of WBC, RBC and PLT count of ApoE^{-/-} mice following treatment with saline and **ZY-P1-PMEA** NPs.

Figure S45. Quantitative analysis of T-Bil, D-Bil and TBA of ApoE^{-/-} mice following treatment with saline and **ZY-P1-PMEA** NPs.

Figure S46. Quantitative analysis of ALT, AST and ALP of ApoE^{-/-} mice following treatment with saline and **ZY-P1-PMEA** NPs.

Figure S47. Quantitative analysis of CREA and UREA of ApoE^{-/-} mice following treatment with saline and **ZY-P1-PMEA** NPs.

Equipment and Methods

Materials and methods

Materials

Bis(tri-tert-butylphosphine)palladium(0) ($\text{Pd}(\text{t-Bu}_3\text{P})_2$), 4,7-Bis(5-bromo-2-thienyl)-2,1,3-benzothiadiazole, Boronic acid and B-[4-[bis(4-methoxyphenyl)amino]phenyl]- were purchased from Adamas Reagent, Ltd. (Shanghai, China). BODIPY 493/503 Green was purchased from Thermo Fisher Scientific. Lyso-blue was purchased from Keygen Biotech Company. All other chemicals and solvents were used as received without further purification.

Characterization

NMR spectra were acquired on a Bruker AVANCE NEO 400 spectrometer. Fluorescence emission spectra were obtained using a Hitach 4700 fluorescence spectrometer. Absorption spectra were obtained on a HITACHI U-2910 spectrometer. High-resolution mass spectra (HRMS) were obtained with a Shimadzu LCMS-IT-TOF (ESI). Infrared spectra were acquired on a FT-IR spectrometer (Perkinelmer Spectrum 3). Particle size and Zeta potential were measured on a Zetasizer Pro (ZSU3200). The observation of cells and tissues was performed on a Leica Stellaris 5 confocal laser scanning microscope (CLSM). The removed aortas and main organs were observed on an Aniview 100 multimodal animal *in vivo* imaging system.

Synthesis of ZY-P1

ZY-P1 is synthesized just by one-step reaction (Figure S1). Under a nitrogen atmosphere, B-[4-[bis(4-methoxyphenyl)amino]phenyl]- (1000 mg, 2.86 mmol), 4,7-Bis(5-bromo-2-thienyl)-2,1,3-benzothiadiazole, Boronic acid (1010 mg, 2.20 mmol), CsF (1000 mg, 6.6 mmol) and $\text{Pd}(\text{t-Bu}_3\text{P})_2$ (56 mg, 0.11 mmol) were put into a 120 mL Schlenk flask and a mixed solution of 18 mL THF and 1.8 mL H_2O was added. The reaction was stirred at 75 °C for 24 h. Afterwards, the solvent was removed by rotary evaporation and the solid was dissolved in dichloromethane (DCM) and purified by flash column chromatography to obtain **ZY-P1**. **ZY-P1** was obtained as a purple solid (1.29 g, yield 62.82 %).

Cytotoxicity of ZY-P1 and NPs

The cytotoxic effects of compound **ZY-P1** and NPs on HeLa and HUVEC cell lines were assessed using the Cell Counting Kit-8 (CCK8). Initially, cells were plated in 96-well culture plates at a density of 5,000 cells per well and allowed to adhere for 24 h. Subsequently, the original medium was removed and replaced with fresh medium containing varying concentrations of the test compound and nanoparticles, followed by an additional 24-h incubation period. Finally, cell viability was determined by performing the CCK8 assay in accordance with the manufacturer's protocol.

Cell imaging of ZY-P1

A 5 μ M solution of **ZY-P1**, prepared in serum-free culture medium, was applied to the cells and incubated for 1 hour. Subsequently, the cells were labeled with BODIPY 493/503 Green fluorescent dye (100 nM) for 30 minutes. Following three PBS washes to remove unbound dye, cellular fluorescence was visualized using CLSM. To evaluate the photostability of **ZY-P1**, HeLa cells were employed as the model cell line and seeded into glass-bottom dishes for 24-hour culture. Subsequently, the **ZY-P1** solution was diluted with serum-free medium to a final concentration of 5 μ M. After adding the solution to the culture system, the cells were incubated for an additional hour. Following three washes with PBS, time-lapse imaging of the stained cells was performed under a CLSM for a duration of 5 minutes, with the time interval set at 5 seconds.

Synthesis of AEMA

2-(azepan-1-yl)ethan-1-ol (4000 mg, 27.9 mmol) and triethylamine (4234.4 mg, 41.9 mmol) were put into a 100 mL flask and dissolved in 40 mL THF. The reaction flask was stirred in an ice bath while 2-methacryloyl chloride (3499.7 mg, 33.5 mmol) was dissolved in 15 mL THF and added dropwise into the flask through a constant pressure funnel. After addition, the ice bath was removed, and the reaction was carried out at 25 $^{\circ}$ C for 24 h. After the reaction, the solution was filtered to remove the precipitates, followed by concentration and the product was purified by flash column chromatography. Finally, 4303.8 mg of pale yellow liquid AEMA was obtained (yield

73.0 %).

Synthesis of PME A

The synthesis of the pH-sensitive monomer AEMA is shown in the supporting information. The synthetic route of the PME A copolymer is shown in Figure S2. Under a nitrogen atmosphere, 2-(methacryloyloxy) ethyl 2-(trimethylammonio) ethyl phosphate (MPC) (5001.3 mg, 16.9 mmol), 4-cyano-4-((phenylcarbonothioyl) thio) pentanoic acid (CTP) (278.5 mg, 0.997 mmol) and azobisisobutyronitrile (AIBN) (65.4 mg, 0.398 mmol) were placed in a 120 mL Schlenk flask, and 15 mL of methanol was added. The reaction was stirred at 60 °C for 24 h. Subsequently, the resulting polymer PMPC was isolated by precipitation with ice ether and dried under vacuum. Under a nitrogen atmosphere, PMPC (999.7 mg, 0.17 mmol), AEMA (500.8 mg, 2.37 mmol), 2-phenylethyl acrylate (PA) (201.2 mg, 1.14 mmol) and AIBN (11.2 mg, 0.068 mmol) were placed in a 120 mL Schlenk flask, and a mixed solution consisting of 5 mL methanol and 5 mL tetrahydrofuran (THF) was added. The reaction was stirred at 60 °C for 36 h. Subsequently, the resulting pH-responsive polymer PME A was isolated by precipitation with ice ether and dried by vacuum.

Preparation of ZY-P1-PME A NPs

The probe-encapsulated PME A nanoparticles (**ZY-P1-PME A NPs**) were synthesized using a nanoprecipitation method. Briefly, 1 mg of **ZY-P1** and 10 mg of PME A were co-dissolved in a 1:1 (v/v) mixture of tetrahydrofuran (THF) and methanol. This organic solution was then rapidly injected into vigorously stirred deionized water (pH 7.4) under continuous stirring for 30 minutes. The resulting nanoparticle suspension was subjected to dialysis against reverse osmosis (RO) (pH 7.4) water for 24 h using a membrane with a molecular weight cutoff (MWCO) of 3.5 kDa. Following purification via ultrafiltration, the nanoparticles were collected, and their probe loading characteristics were quantitatively assessed by calculating both the probe loading content (PLC) and drug loading efficiency (PLE) using standard formulas.

$$PLC = \frac{\text{weight of loaded ZY - P1}}{\text{weight of polymer and loaded ZY - P1}}$$

$$PLE = \frac{\text{weight of loaded ZY - P1}}{\text{weight of added ZY - P1}}$$

For comparative analysis, blank PMEAs nanoparticles (**PMEA NPs**) were fabricated following an identical preparation protocol, omitting the incorporation of **ZY-P1**. The hydrodynamic diameter and surface charge characteristics of both nanoparticle formulations were determined through dynamic light scattering (DLS) analysis. Furthermore, nanoparticle morphology was examined by transmission electron microscopy (TEM), with samples negatively stained using phosphotungstic acid to enhance contrast.

Spectrophotometric experiments

A DMSO stock solution of **ZY-P1** was prepared (5 mM). The concentration of **ZY-P1** remains the same (5 μM) in all spectroscopic measurements.

pH responsiveness of NPs

To explore the pH sensitivity of nanoparticles to acidic pH, nanoparticles were dissolved in PBS at different pH values (6.5 or 7.4), and their particle size and Zeta potential were measured by DLS. TEM was used to reflect the morphology changes.

The release behavior of **ZY-P1** from nanoparticles was also studied. Two milliliters of **ZY-P1-PMEA NPs** solution ($1 \text{ mg}\cdot\text{mL}^{-1}$) was placed into a dialysis bag (MWCO = 3500). Under dark conditions, the dialysis bag was immersed in 20 mL of PBS with different pH values (7.4 or 6.5) at 37 °C with continuous shaking. Two milliliters of PBS was taken at preselected time points, and 2 mL of fresh PBS was added. The obtained PBS was lyophilized and further dissolved in 2 mL DMSO to measure its absorbance at 546 nm.

Anti-protein adhesion properties of NPs

A mixed solution of bovine serum albumin (BSA) and **ZY-P1-PMEA NPs** was prepared with PBS, and the final concentrations of **ZY-P1-PMEA NPs** and BSA were $1 \text{ mg}\cdot\text{mL}^{-1}$ and $2 \text{ mg}\cdot\text{mL}^{-1}$, respectively. The particle size and Zeta potential of the mixed solution were recorded after incubation for different time intervals.

Cell culture

HeLa cells and HUVEC cells were cultured in DMEM medium supplemented with 100 units per mL penicillin, 100 $\mu\text{g}\cdot\text{mL}^{-1}$ streptomycin and 10 % (v/v) fetal bovine serum (FBS). Cells were cultured in a humidified atmosphere with 5 % CO_2 at 37 °C.

Cellular imaging of ZY-P1-PMEA NPs

HeLa cells were chosen as a cell model to study the cellular endocytosis of **ZY-P1-PMEA** NPs. Cells with a density of 5000 were seeded in a 96-well plate and incubated for 24 h. **ZY-P1-PMEA** NPs were added at a **ZY-P1** concentration of 5 μM and incubated at 37 °C for periods ranging from 30 min to 4 h. The absorbance of the supernatant at 480 nm was measured on a microplate reader.

In addition, **ZY-P1-PMEA** NPs solution diluted with culture medium was added at a **ZY-P1** final concentration of 5 μM , and the cells were cultured for 1 h, 2 h, 4 h and 6 h, respectively. Then, the cells were stained with BODIPY 493/503 Green (100 nM) for 30 min. After washing with PBS for three times, the cells were observed by CLSM. To evaluate the photostability of **ZY-P1-PMEA** NPs, HeLa cells were first plated in glass-bottom dishes and allowed to adhere for 24 h. The cells were then treated with a 5 μM solution of **ZY-P1** prepared in serum-free medium and incubated for 6 h. After washing with PBS for three times to remove residual compound, time-lapse imaging was conducted using CLSM. Fluorescence signals were captured at 5-second intervals over a 5-minute scanning period to monitor photobleaching behavior.

In glass-bottom dishes, HeLa cells were incubated for 24 h to further study the LDs-specific imaging performance of **ZY-P1-PMEA** NPs. Afterwards, cells were pretreated with oleic acid (20 μM) for 2 h, follow by staining with **ZY-P1** (5 μM) for 2 h. Afterwards, cells were further stained with MitoTracker Blue or LysoTracker Green at a concentration of 1 μM for 0.5 h. Cells were treated three times with PBS before observation by CLSM.

***In Vivo* fluorescence imaging and biocompatibility of ZY-P1-PMEA NPs**

All animal experiments were approved by the medical ethics committee of Sichuan University (20220602005) and strictly complied with relevant national regulations. 13

ApoE^{-/-} mice were randomly divided into three groups and feeding with a high-fat diet for 14 weeks. ApoE^{-/-} mice were administered saline, **ZY-P1**, and **ZY-P1-PMEA** NPs respectively via tail vein injection at a dose of 10 mg/kg body weight. After 24 h, the aortic arch of the mice was subjected to fluorescence imaging using an *in vivo* imaging system. Subsequently, blood samples were collected, followed by euthanasia of the mice. The aortic arch, heart, liver, spleen, lungs, and kidneys were then dissected and harvested.

***In Vivo* pharmacokinetic analysis**

Fasted ApoE^{-/-} mice were randomly divided into 2 groups (n = 3). The mice received tail vein injections of either **ZY-P1** or **ZY-P1-PMEA** NPs at a dose of 10 mg/kg. Blood samples were subsequently collected at various time points. Blood was collected into heparin-containing tubes and centrifuged (3000 rpm, 10 min) to obtain the upper plasma layer. Approximately 10 μL of plasma was mixed with a solution of EA and H₂O, and the fluorescence intensity excited at 546 nm was measured to determine the probe concentration.

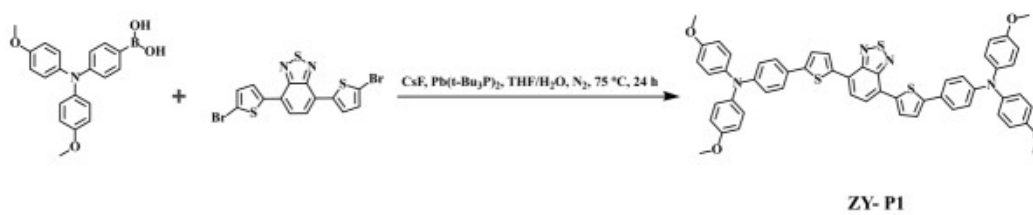


Figure S1. Synthetic route of **ZY-P1**.

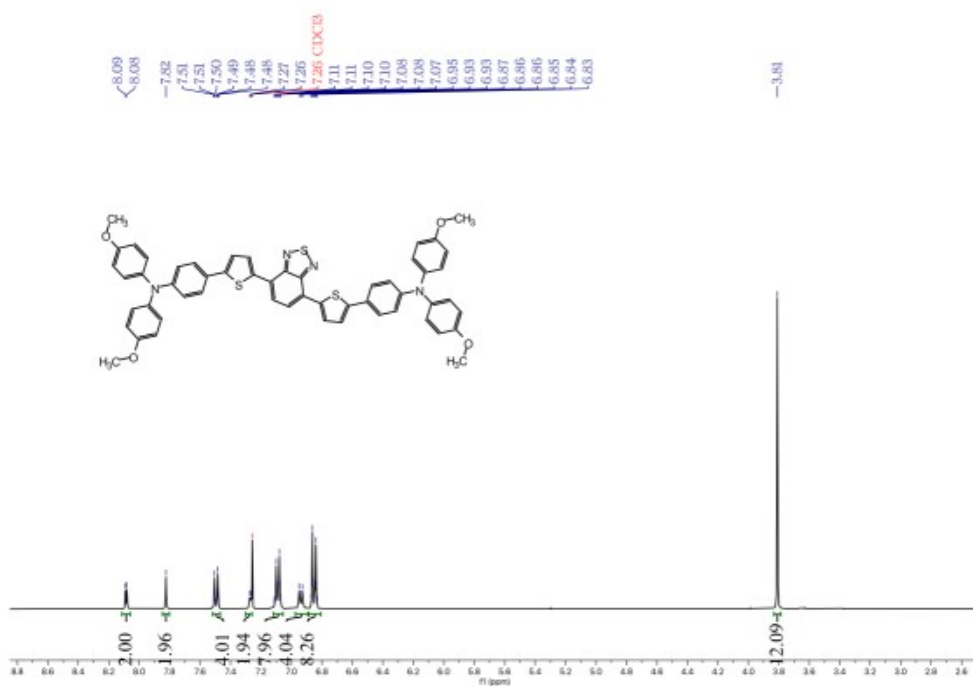


Figure S2. ^1H NMR spectrum of **ZY-P1** in CDCl_3 .

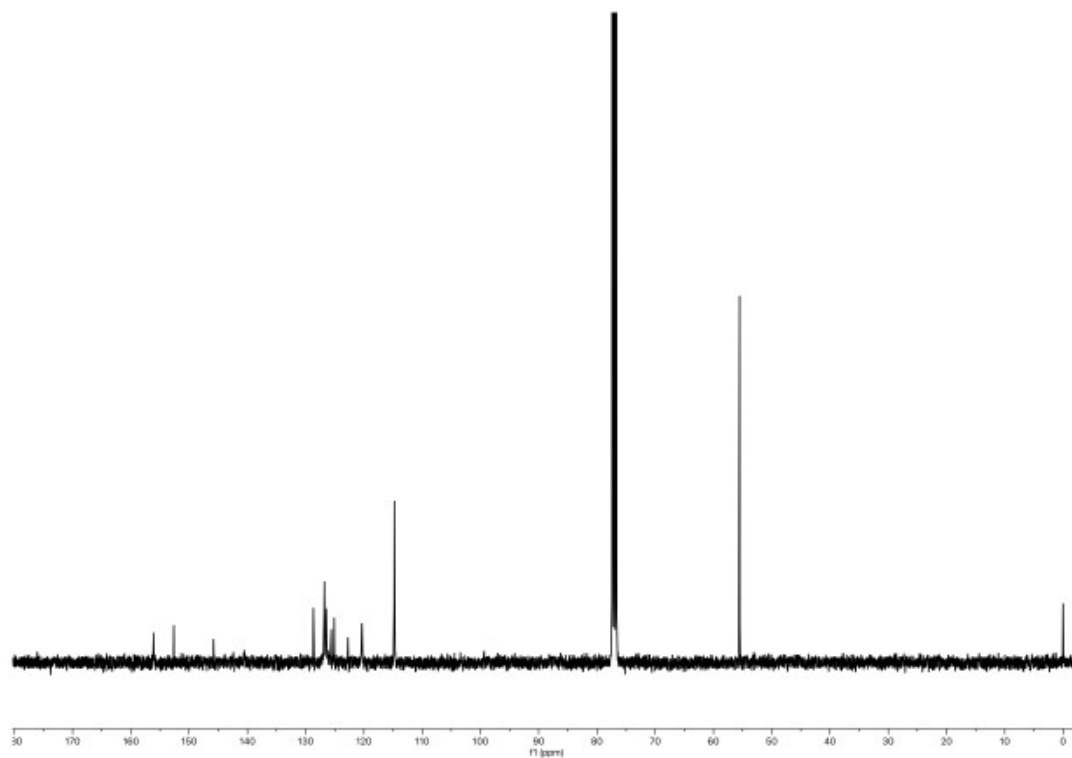


Figure S3. ^{13}C NMR spectrum of **ZY-P1** in CDCl_3 .

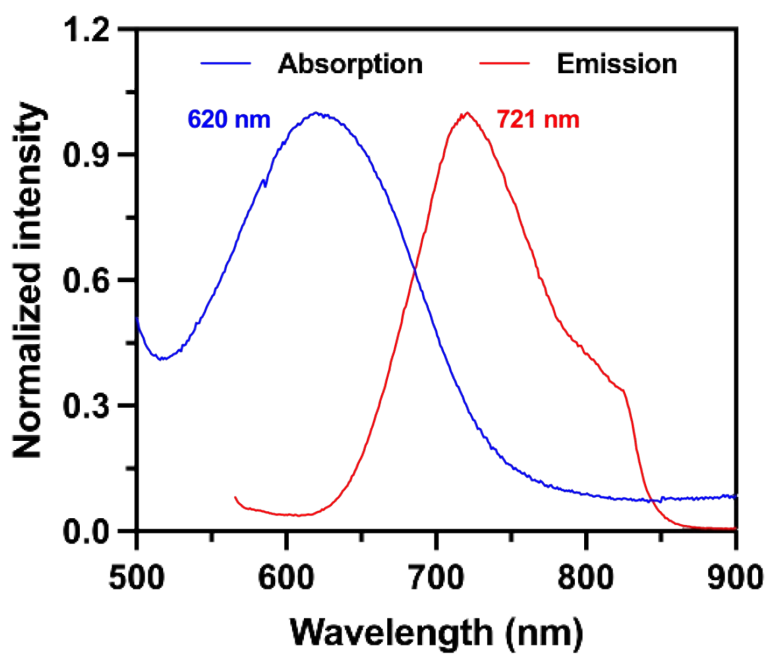


Figure S4. Normalized absorption and emission spectrum of **ZY-P1** in PBS ($5\ \mu\text{M}$, $\lambda_{\text{ex}} = 546\ \text{nm}$).

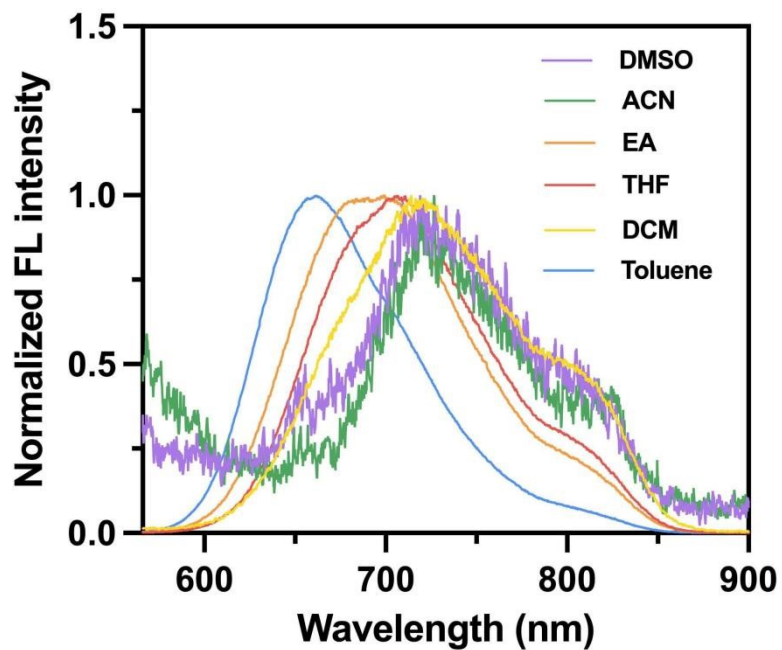


Figure S5. Emission spectra of ZY-P1 in different solvents (5 μM , $\lambda_{\text{ex}} = 546 \text{ nm}$).

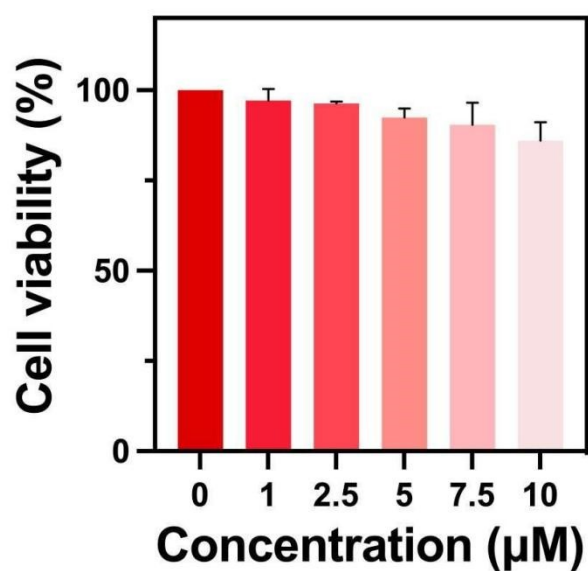


Figure S6. Relative cell viability of HeLa cells co-cultured with different concentrations of ZY-P1 for 24 h.

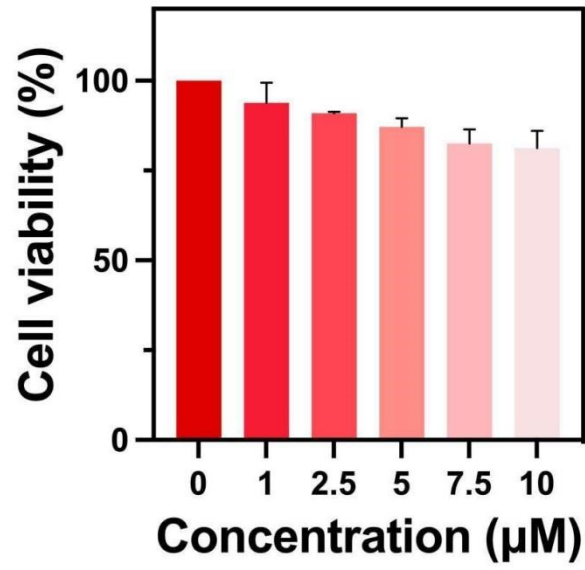


Figure S7. Relative cell viability of HUVEC cells co-cultured with different concentrations of **ZY-P1** for 24 h.

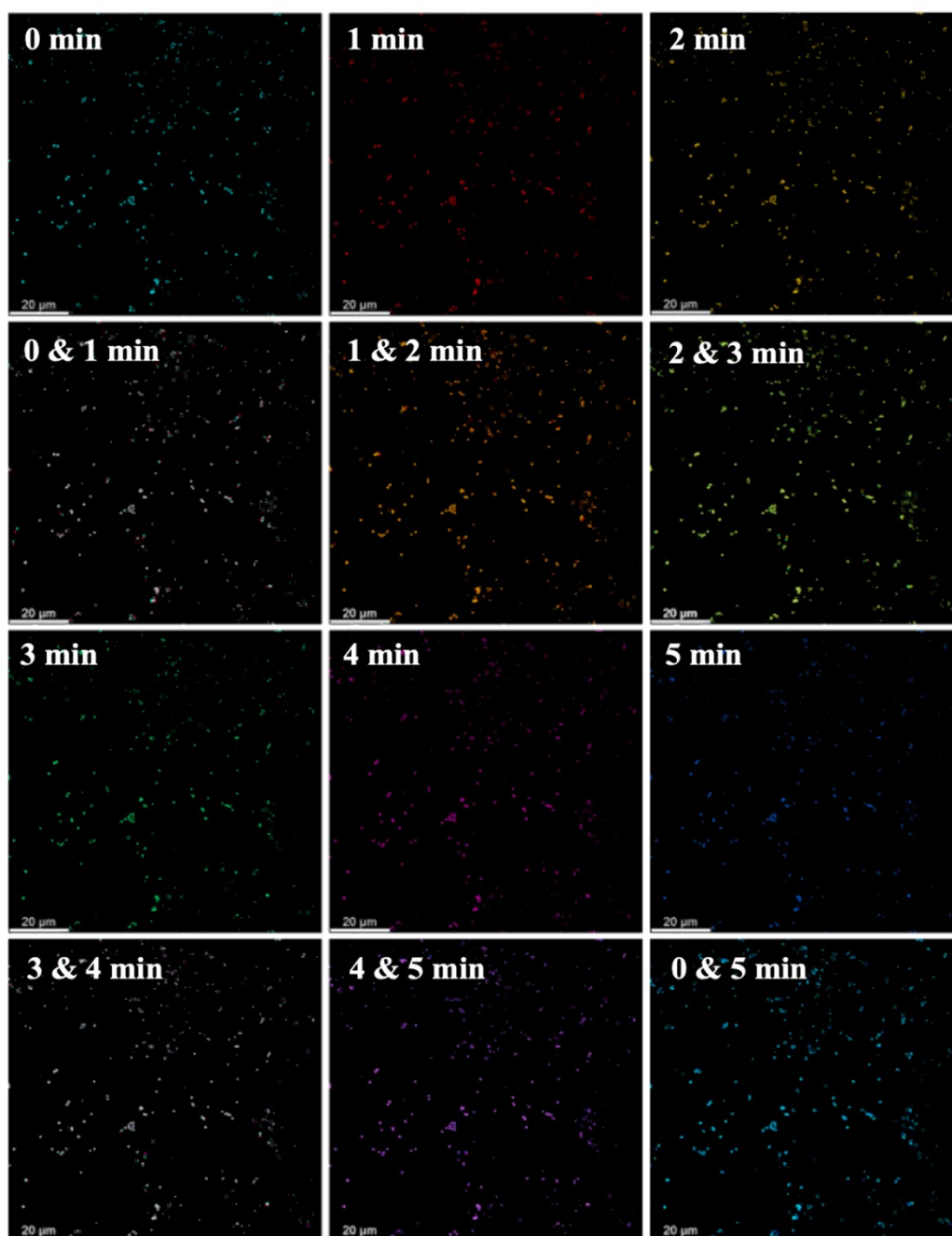


Figure S8. Temporal scanning images of HeLa cells stained with ZY-P1 ($\lambda_{\text{ex}} = 546 \text{ nm}$, $\lambda_{\text{em}} = 600\text{-}700 \text{ nm}$). Time = 5 min. Scale bar = 20 μm .

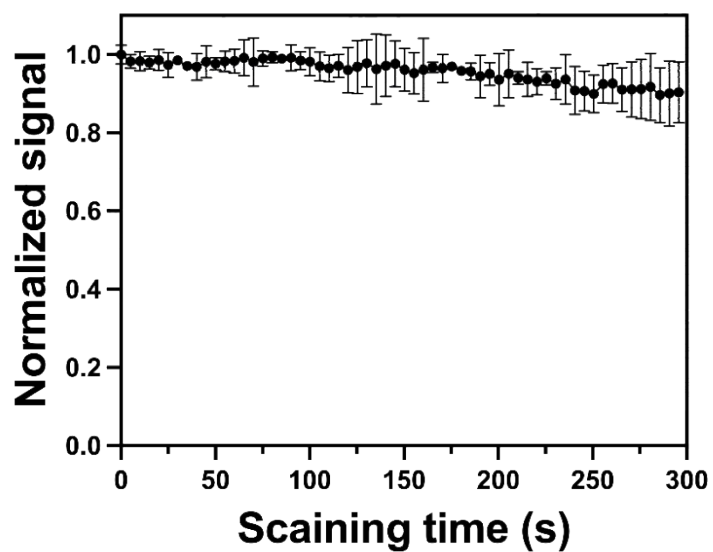


Figure S9. Remaining fluorescence intensity of HeLa cells staining with **ZY-P1** (A, $\lambda_{\text{ex}} = 546 \text{ nm}$, $\lambda_{\text{em}} = 600\text{-}700 \text{ nm}$). Emission signals were normalized to the intensity at the beginning of scanning.

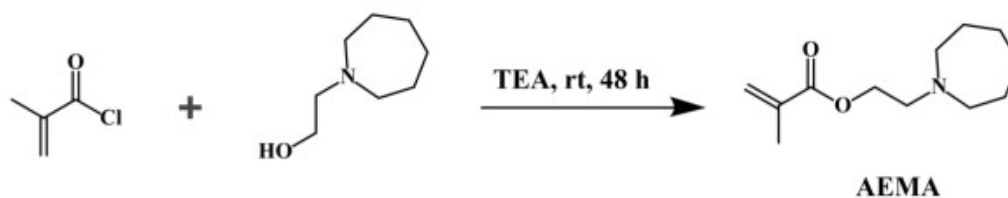


Figure S10. Synthetic route of **AEMA**.

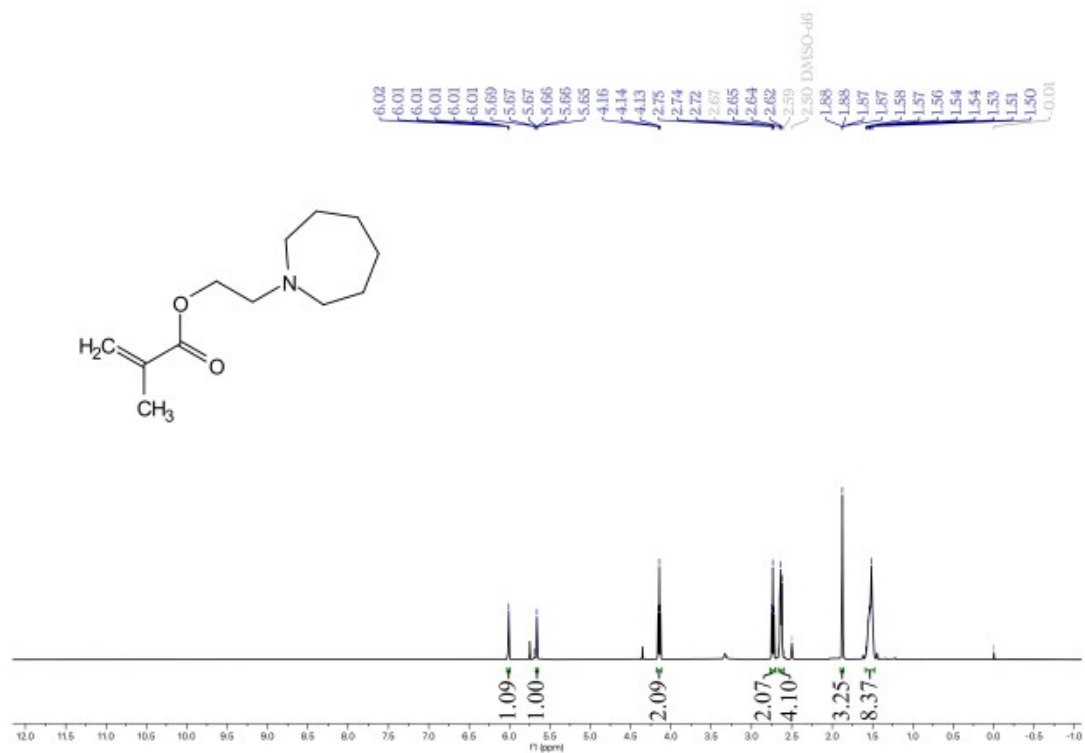


Figure S11. ^1H NMR spectrum of AEMA in $\text{DMSO-}d_6$.

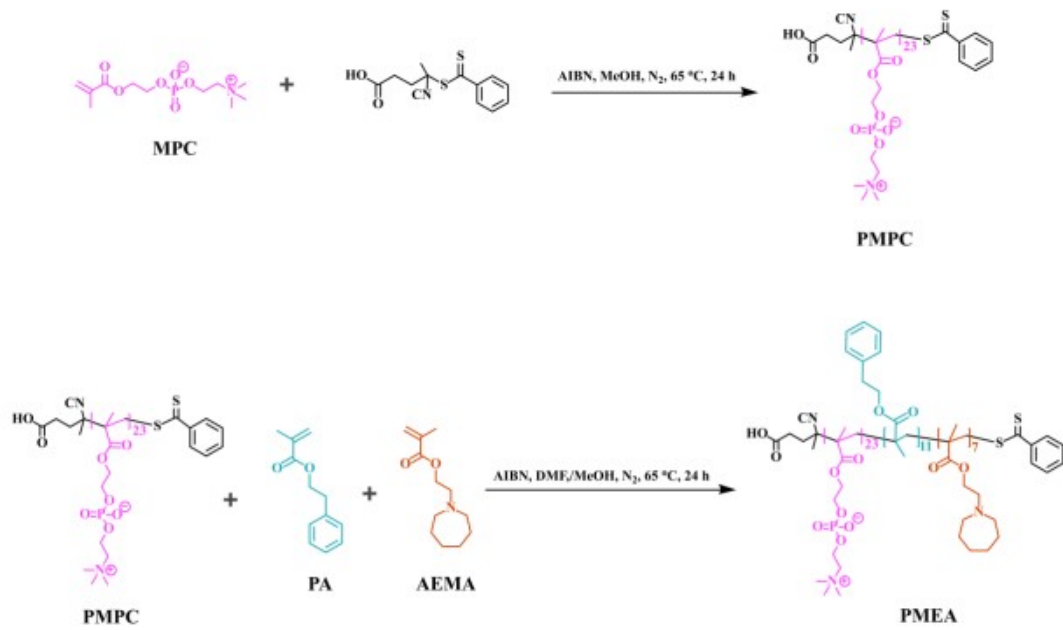


Figure S12. Synthetic route of PMEAs.

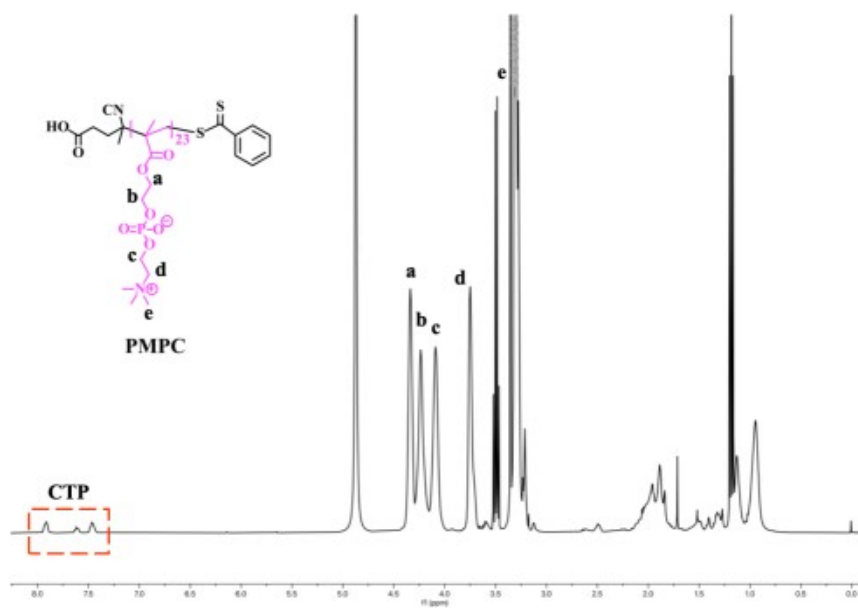


Figure S13. ^1H NMR spectrum of PMPC in CD_3OD .

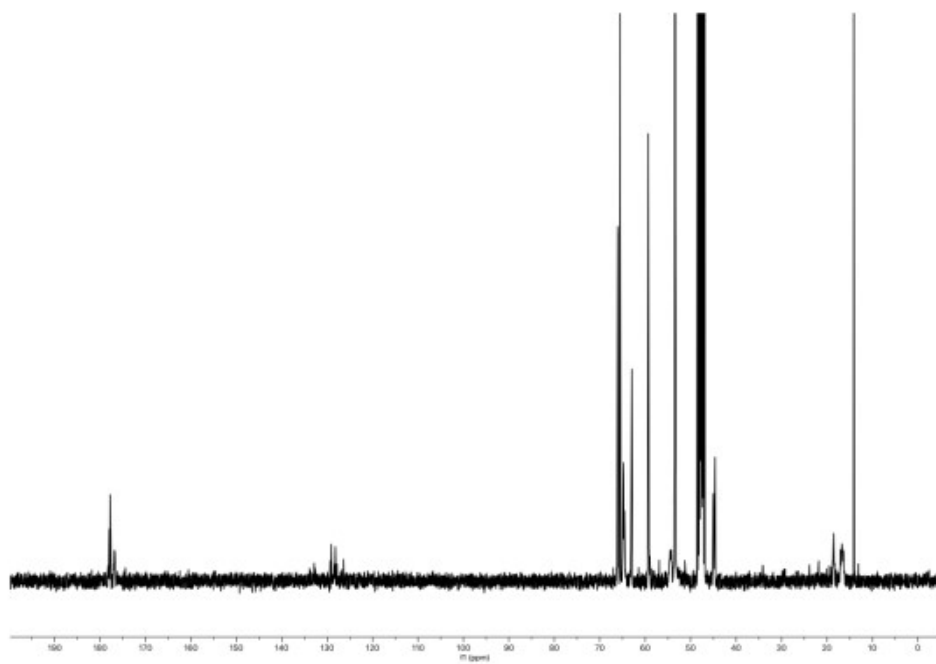


Figure S14. ^{13}C NMR spectrum of PMPC in CD_3OD .

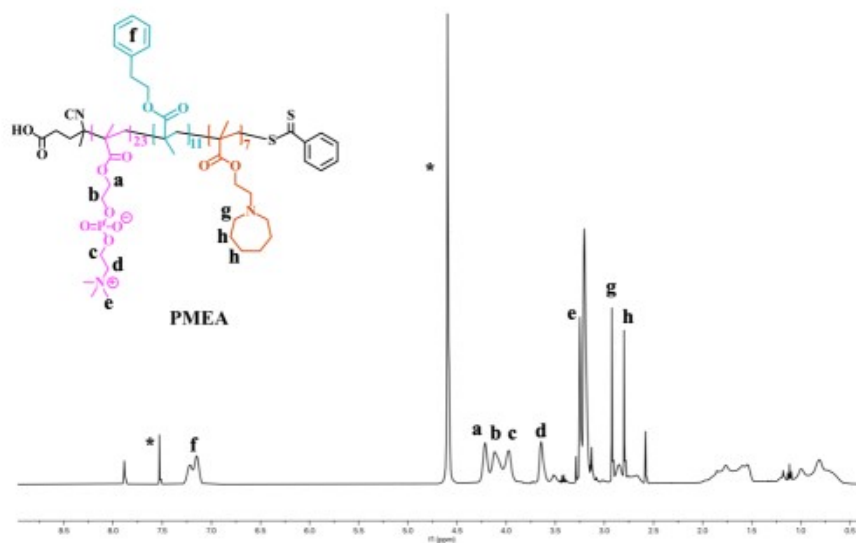


Figure S15. ¹H NMR spectrum of PME A in CD₃OD : CDCl₃ = 1:1 (V/V).

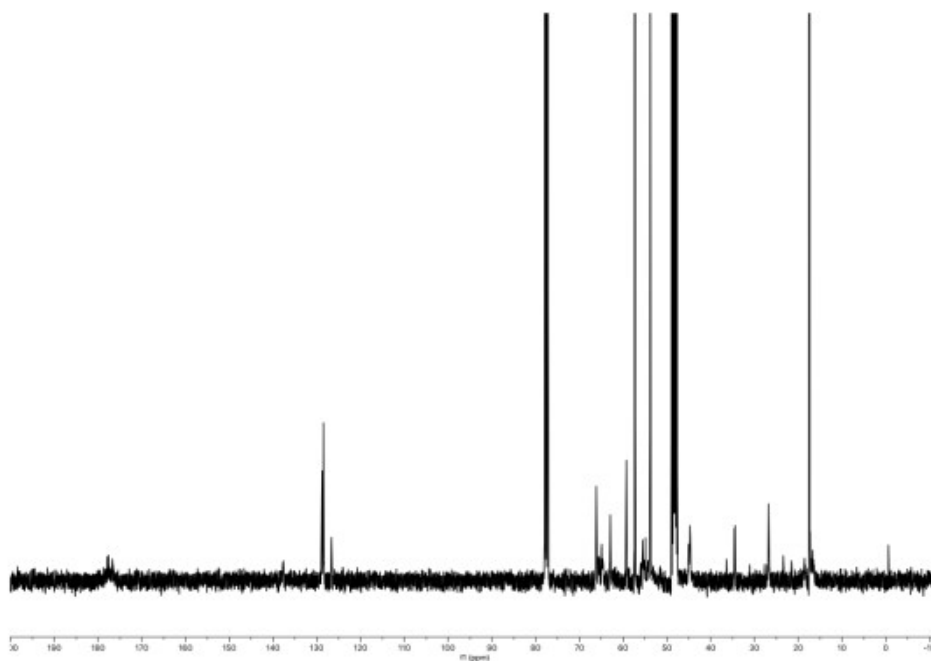


Figure S16. ¹³C NMR spectrum of PME A in CD₃OD : CDCl₃ = 1:1 (V/V).

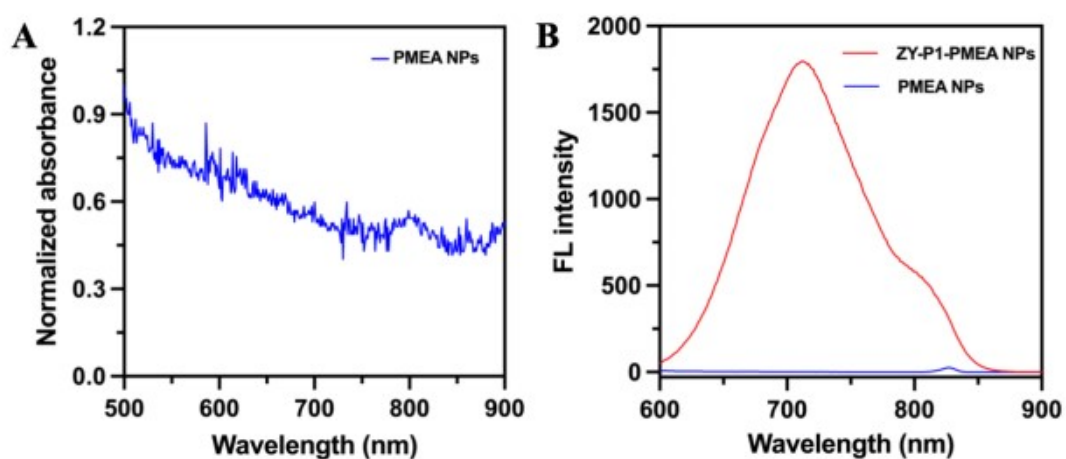


Figure S17. Photophysical studies of NPs. (A) Normalized absorption spectrum of **PMEA** NPs in PBS (NPs = $0.30 \text{ mg}\cdot\text{mL}^{-1}$). (B) Emission spectrum of **PMEA** NPs and **ZY-P1-PMEA** NPs in PBS (NPs = $0.30 \text{ mg}\cdot\text{mL}^{-1}$, $5 \mu\text{M}$, $\lambda_{\text{ex}} = 546 \text{ nm}$).

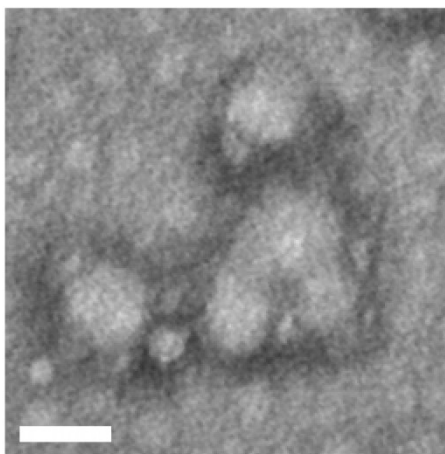


Figure S18. TEM image of **ZY-P1-PMEA** NPs at pH 6.5 (Scale bar = 50 nm).

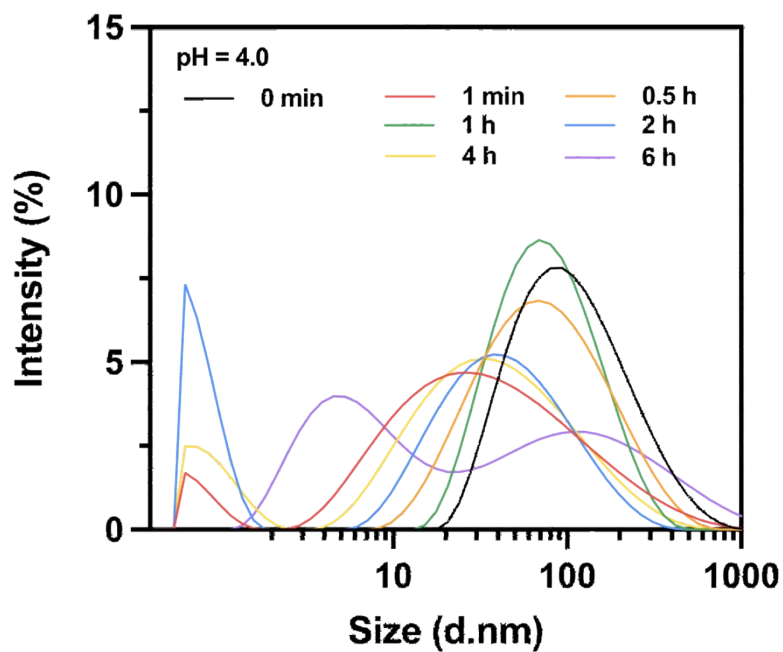


Figure S19. Particle size variation of ZY-P1-PMEA NPs at different time points (pH = 4.0).

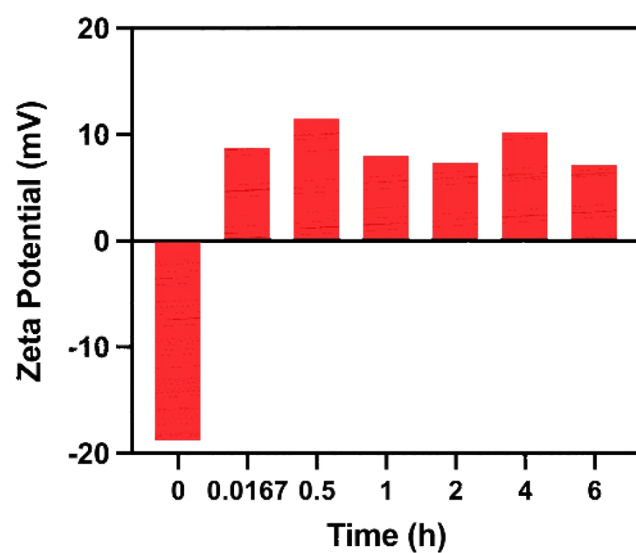


Figure S20. Zeta potential variation of ZY-P1-PMEA NPs at different time points (pH = 4.0).

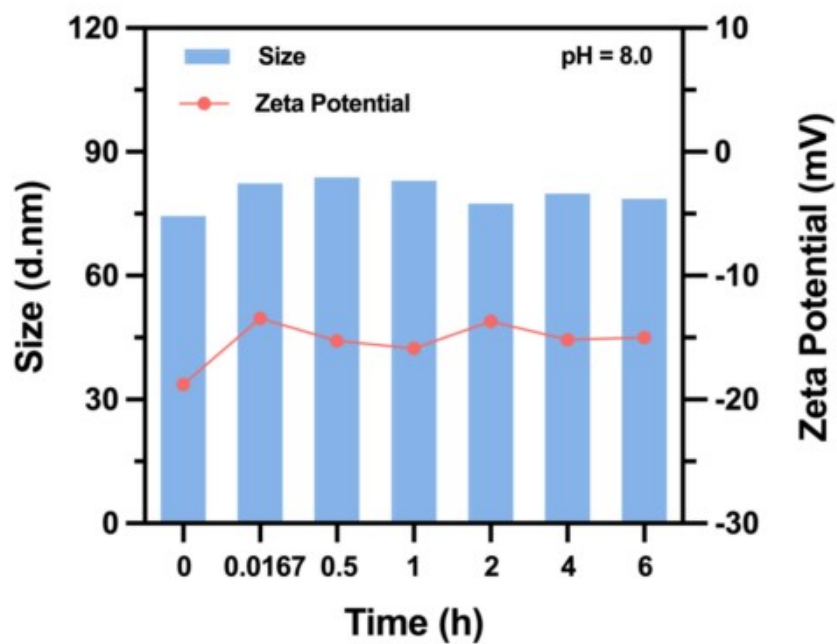


Figure S21. Particle size variation and Zeta potential variation of ZY-P1-PMEA NPs at pH 8.

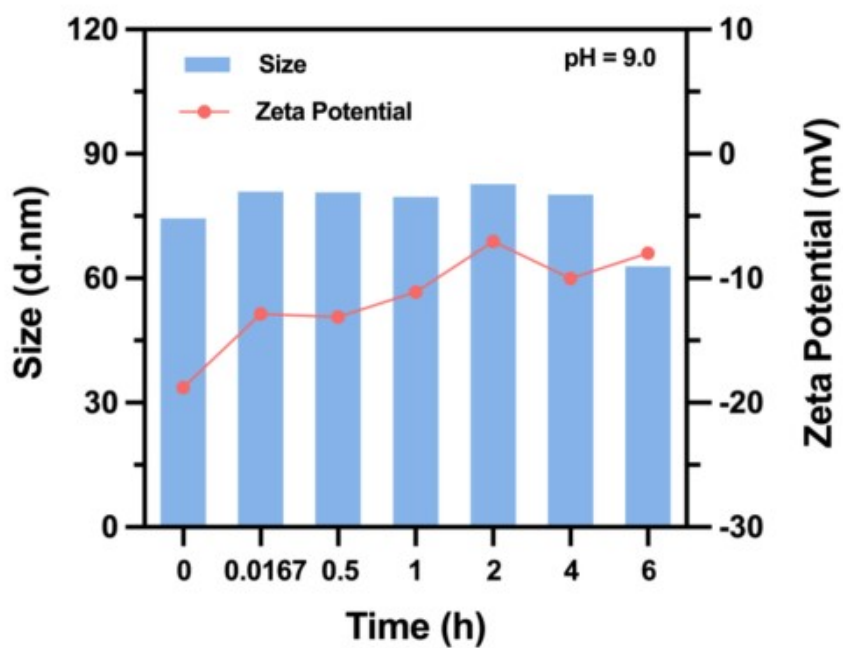


Figure S22. Particle size variation and Zeta potential variation of ZY-P1-PMEA NPs at pH 9.

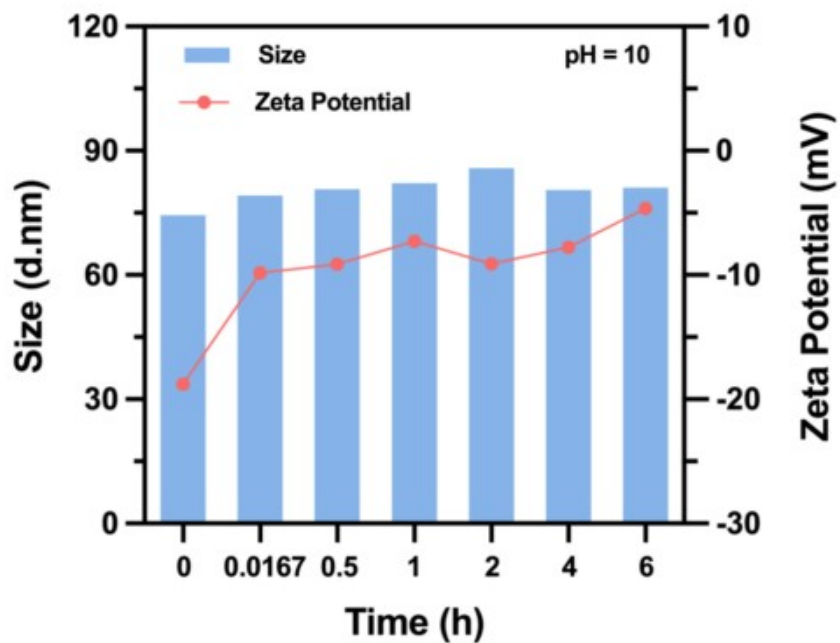


Figure S23. Particle size Variation and Zeta potential variation of **ZY-P1-PMEA** NPs at pH 10.

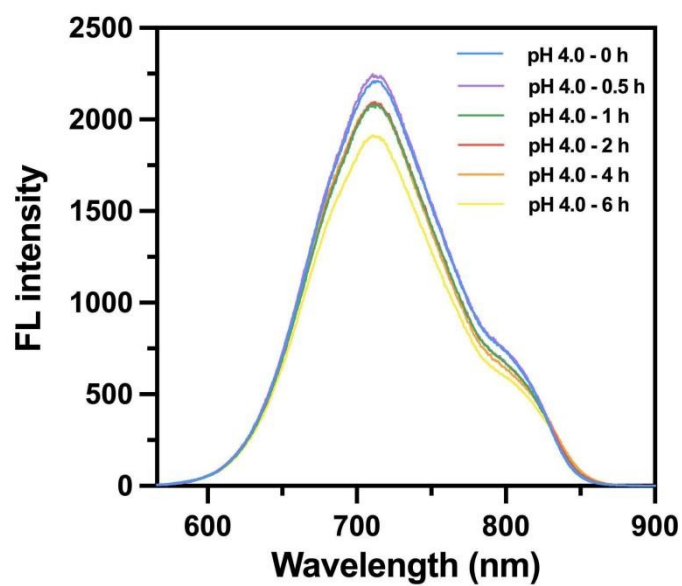


Figure S24. Emission spectra of **ZY-P1-PMEA** NPs in PBS (pH = 4.0) at different time points (**ZY-P1** = 5 μ M, λ_{ex} = 546 nm).

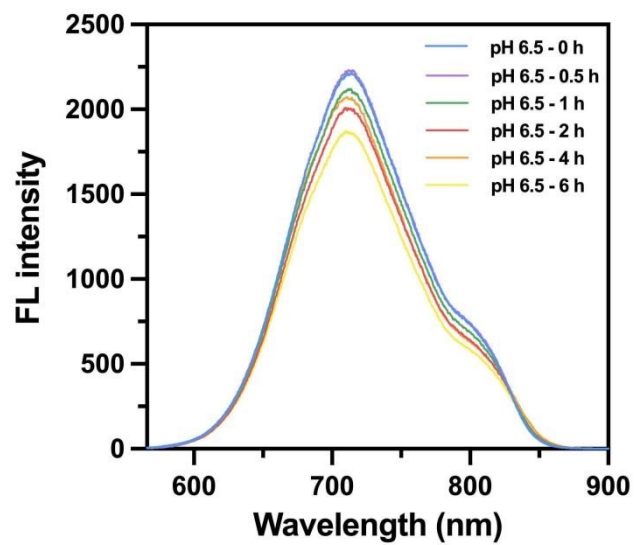


Figure S25. Emission spectra of **ZY-P1-PMEA** NPs in PBS (pH = 6.5) at different time points (**ZY-P1** = 5 μ M, λ_{ex} = 546 nm).

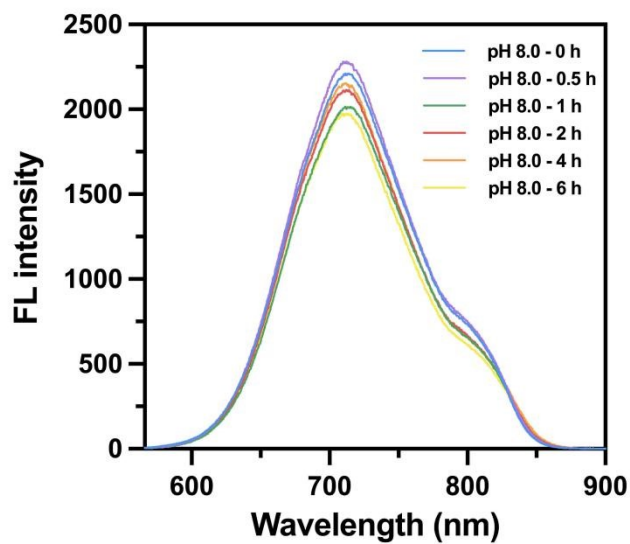


Figure S26. Emission spectra of **ZY-P1-PMEA** NPs in PBS (pH = 8.0) at different time points (**ZY-P1** = 5 μ M, λ_{ex} = 546 nm).

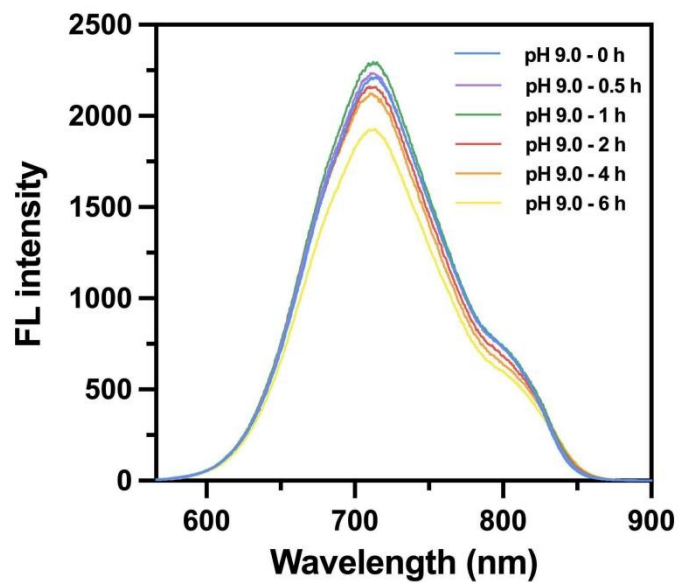


Figure S27. Emission spectra of **ZY-P1-PMEA** NPs in PBS (pH = 9.0) at different time points (**ZY-P1** = 5 μ M, λ_{ex} = 546 nm).

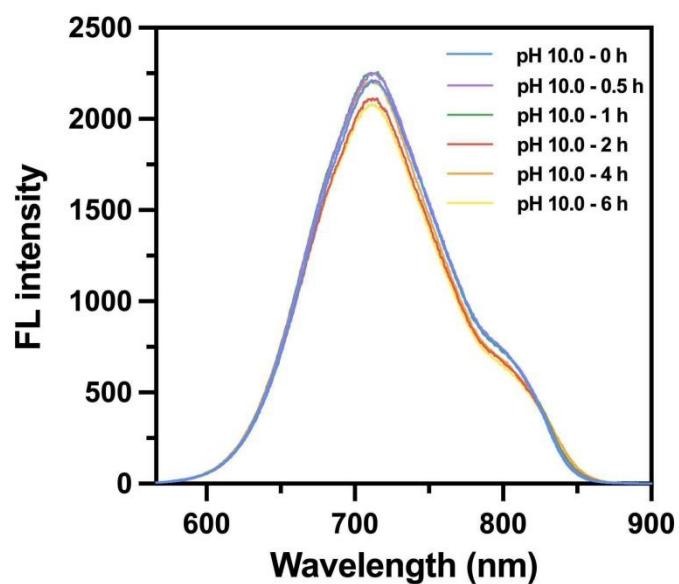


Figure S28. Emission spectra of **ZY-P1-PMEA** NPs in PBS (pH = 10.0) at different time points (**ZY-P1** = 5 μ M, λ_{ex} = 546 nm).

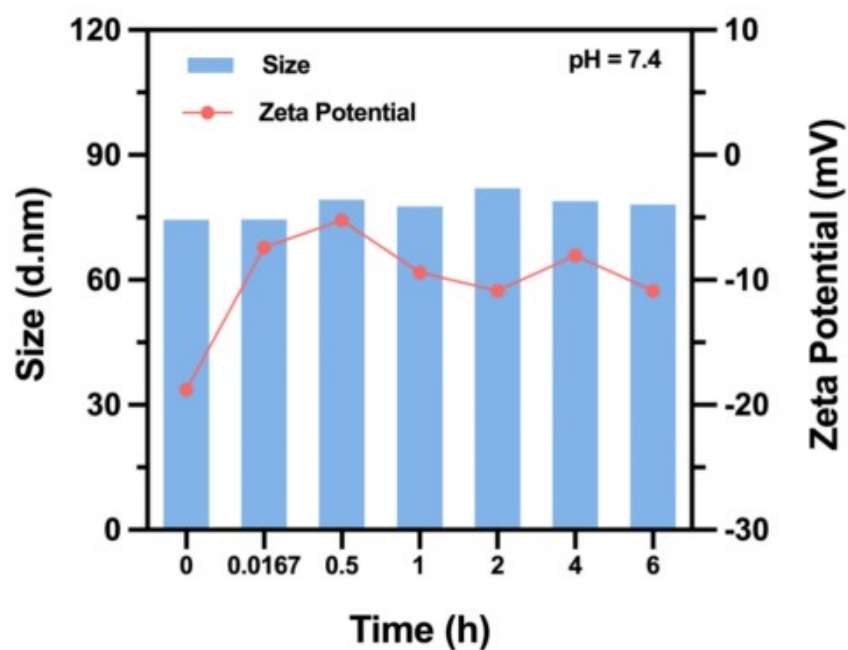


Figure S29. Particle size variation of and Zeta potential variation of ZY-P1-PMEA NPs incubation with $2 \text{ mg}\cdot\text{mL}^{-1}$ BSA solution.

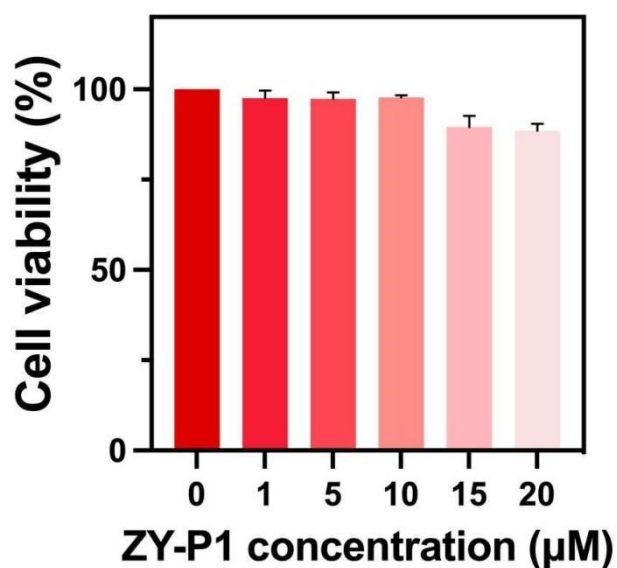


Figure S30. Relative cell viability of HeLa cells co-cultured with different concentrations of ZY-P1-PMEA NPs for 24 h.

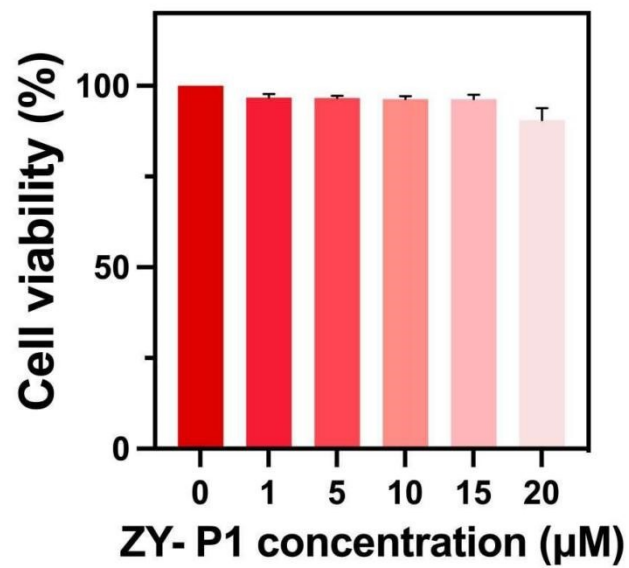


Figure S31. Relative cell viability of HUVEC cells co-cultured with different concentrations of ZY-P1-PMEA NPs for 24 h.

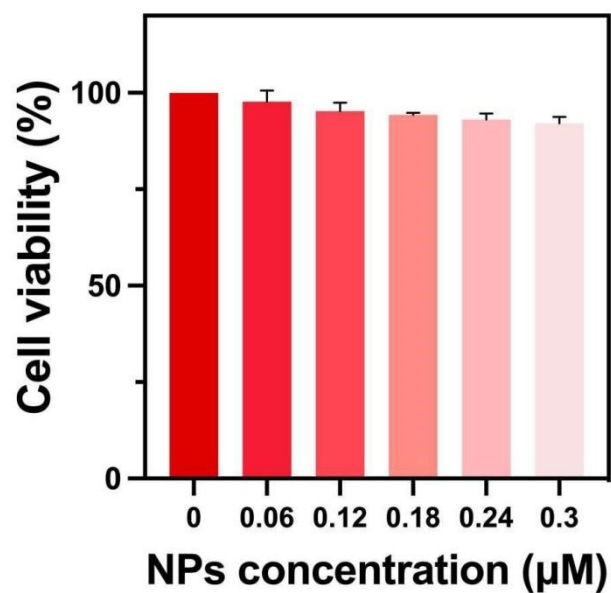


Figure S32. Relative cell viability of HeLa cells co-cultured with different concentrations of PMEAs NPs for 24 h.

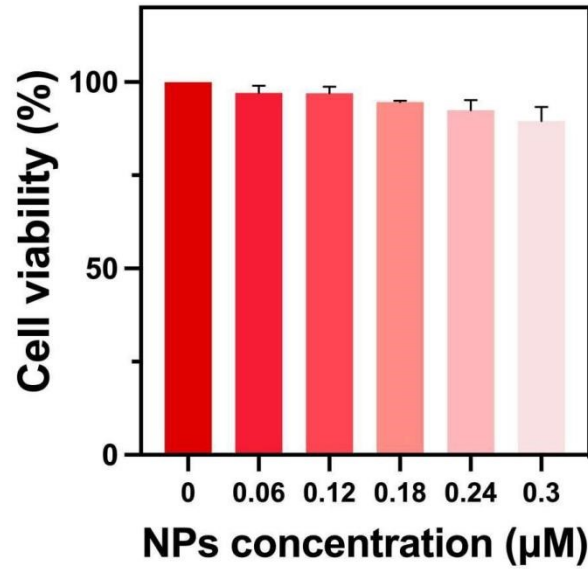


Figure S33. Relative cell viability of HUVEC cells co-cultured with different concentrations of PME A NPs for 24 h.

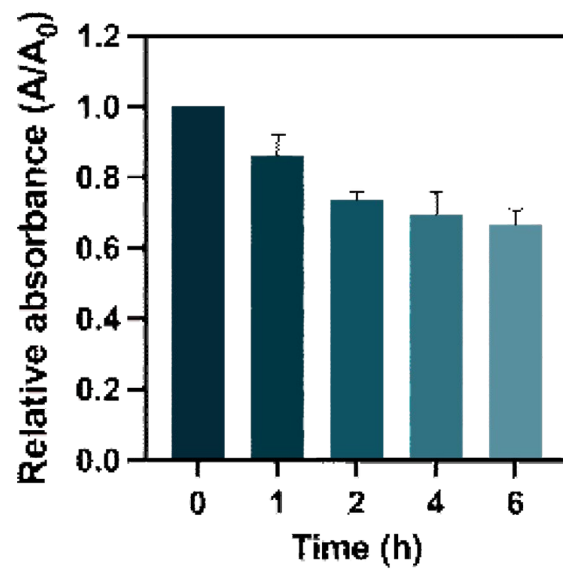


Figure S34. Cellular uptake of ZY-P1-PME A NPs: the ratio of the absorbance (A) of culture medium after incubation for different time intervals to the initial value (A_0).

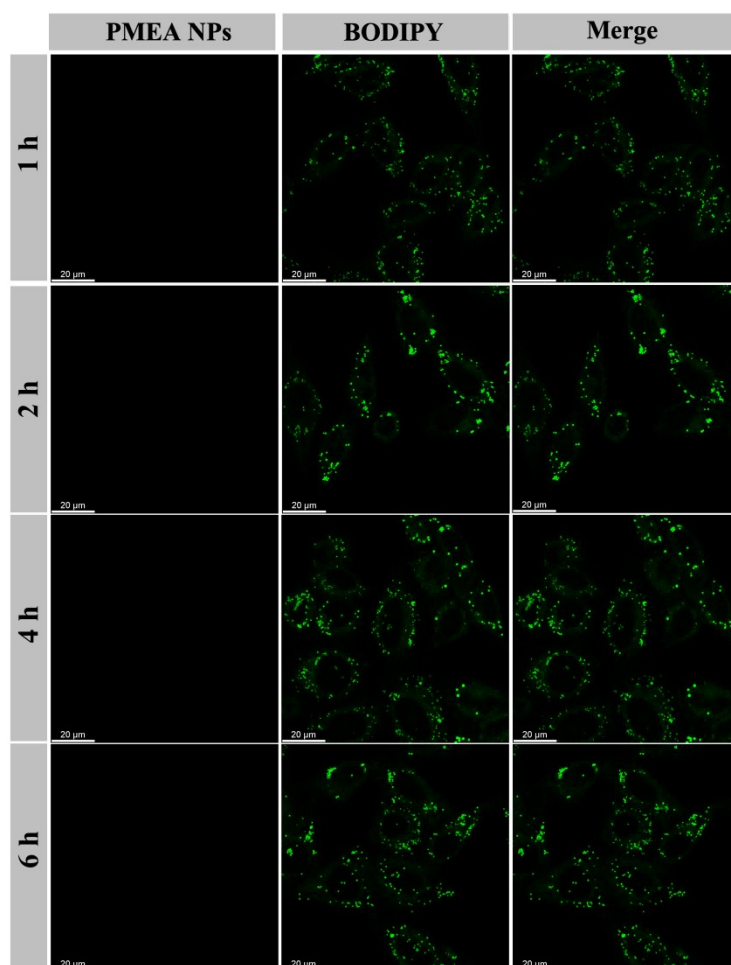


Figure S35. Colocalization imaging of HeLa cells stained with BODIPY 493/503 Green (100 nM, $\lambda_{\text{ex}} = 488 \text{ nm}$, $\lambda_{\text{em}} = 500\text{-}550 \text{ nm}$) and **PMEA NPs** (PMEA NPs = 0.30 $\text{mg}\cdot\text{mL}^{-1}$, $\lambda_{\text{ex}} = 546 \text{ nm}$, $\lambda_{\text{em}} = 600\text{-}700 \text{ nm}$) for 1, 2, 4, and 6 h. All the scale bars = 20 μm .

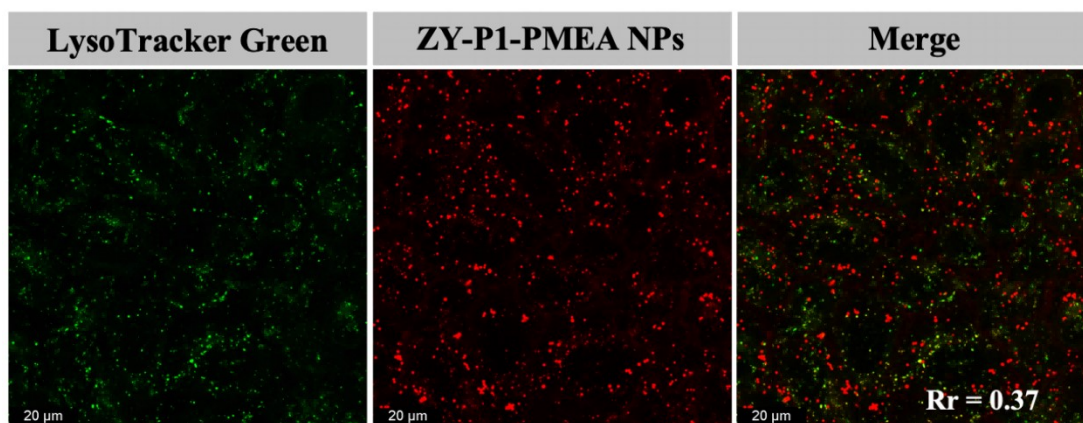


Figure S36. Colocalization imaging of HeLa cells stained with LysoTracker Green (1 μM , $\lambda_{\text{ex}} = 405 \text{ nm}$, $\lambda_{\text{em}} = 430\text{-}480 \text{ nm}$) and ZY-P1-PMEA NPs (ZY-P1 = 5 μM , $\lambda_{\text{ex}} = 546 \text{ nm}$, $\lambda_{\text{em}} = 600\text{-}700 \text{ nm}$). All the scale bars = 20 μm .

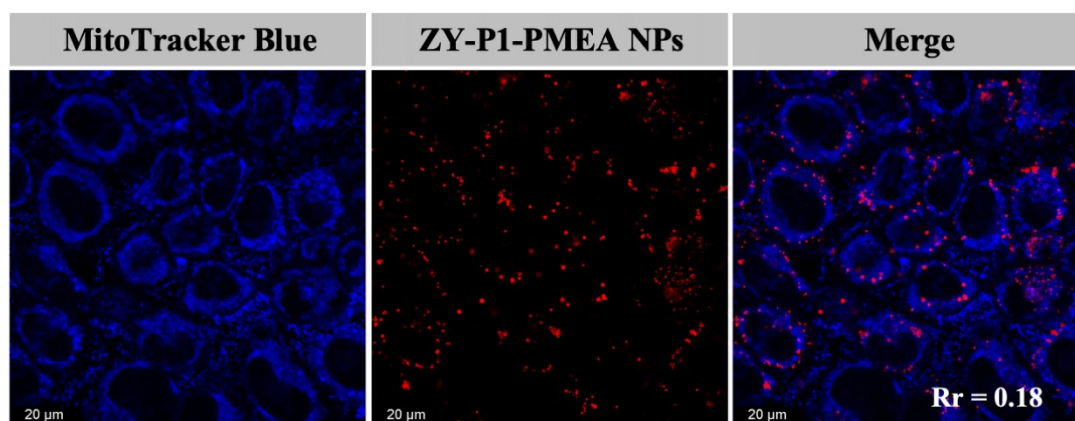


Figure S37. Colocalization imaging of HeLa cells stained with MitoTracker Blue (1 μM , $\lambda_{\text{ex}} = 405 \text{ nm}$, $\lambda_{\text{em}} = 430\text{-}480 \text{ nm}$) and ZY-P1-PMEA NPs (ZY-P1 = 5 μM , $\lambda_{\text{ex}} = 546 \text{ nm}$, $\lambda_{\text{em}} = 600\text{-}700 \text{ nm}$). All the scale bars = 20 μm .

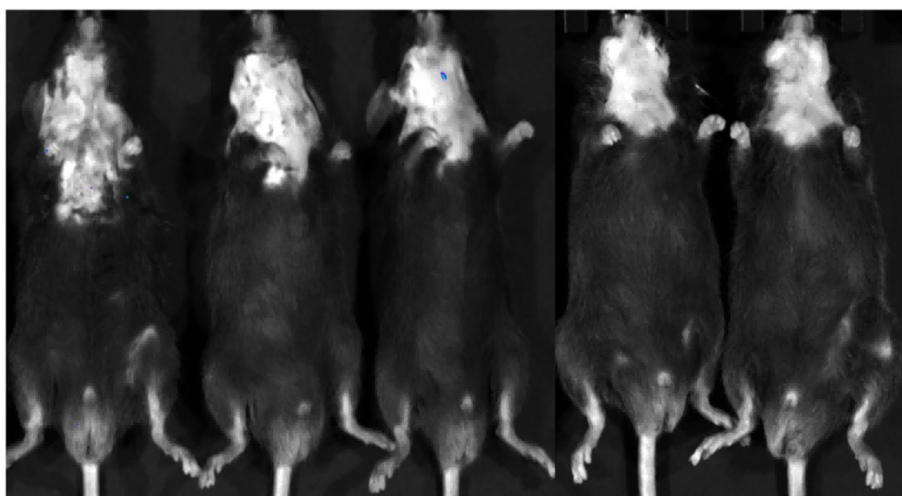


Figure S38. *In vivo* fluorescence image of ApoE^{-/-} mice following tail vein injection of saline.

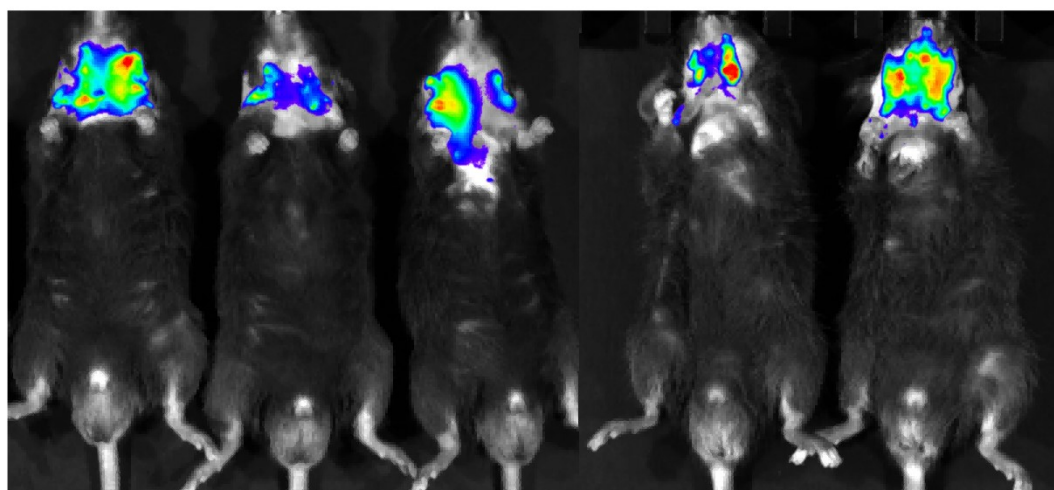


Figure S39. *In vivo* fluorescence image of ApoE^{-/-} mice following tail vein injection of ZY-P1-PMEA NPs.

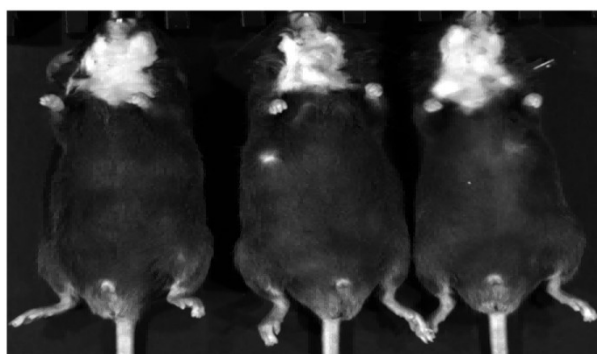


Figure S40. *In vivo* fluorescence image of ApoE^{-/-} mice following tail vein injection of free ZY-P1.

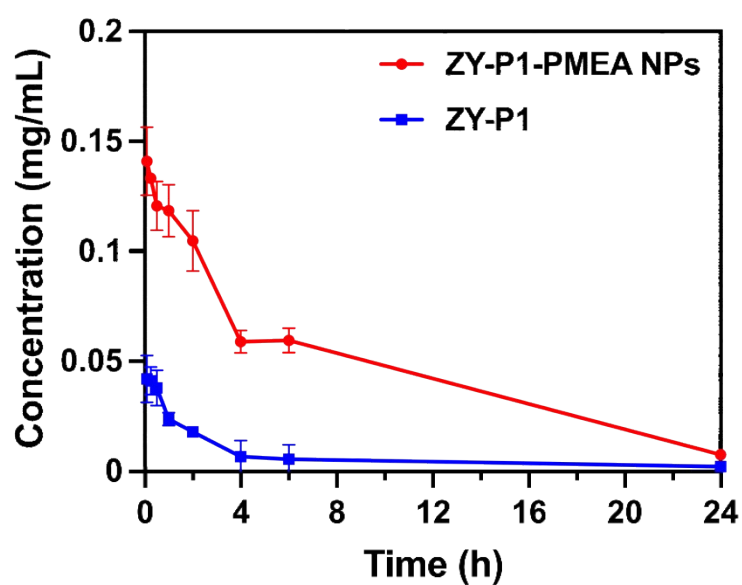


Figure S41. Pharmacokinetic analysis. Plasma concentration-time profiles of probe following a single intravenous injection of free ZY-P1 and ZY-P1-PMEA NPs.

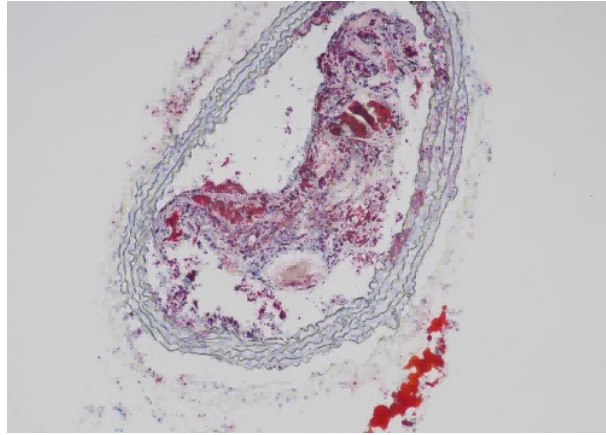


Figure S42. Oil Red O staining of aortic sections from ApoE^{-/-} mice. Scale bar = 100 μ m.

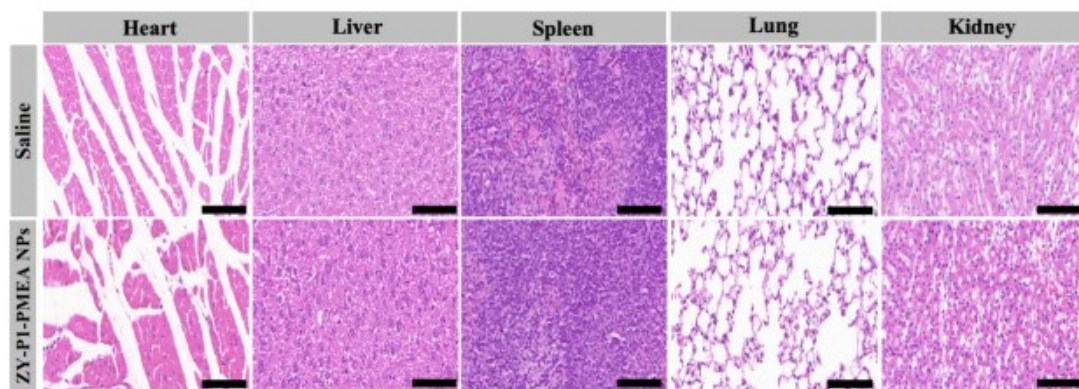


Figure S43. H&E staining of major organs sections from ApoE^{-/-} mice treated with saline or ZY-P1-PMEA NPs. All the scale bars = 100 μ m.

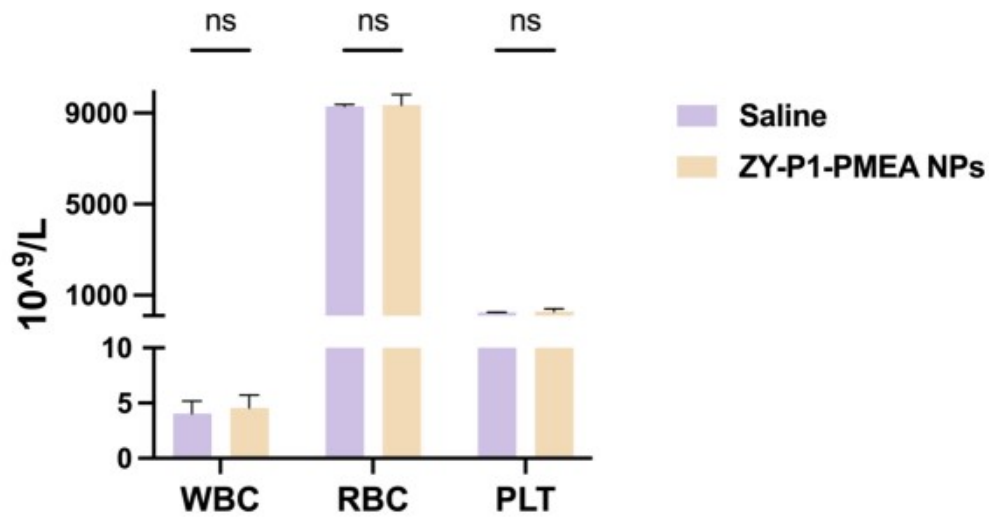


Figure S44. Quantitative analysis of WBC, RBC and PLT count of *AopE*^{-/-} mice following treatment with saline and **ZY-P1-PMEA** NPs. WBC = White Blood Cell, RBC = Red Blood Cell, PLT = Platelet.

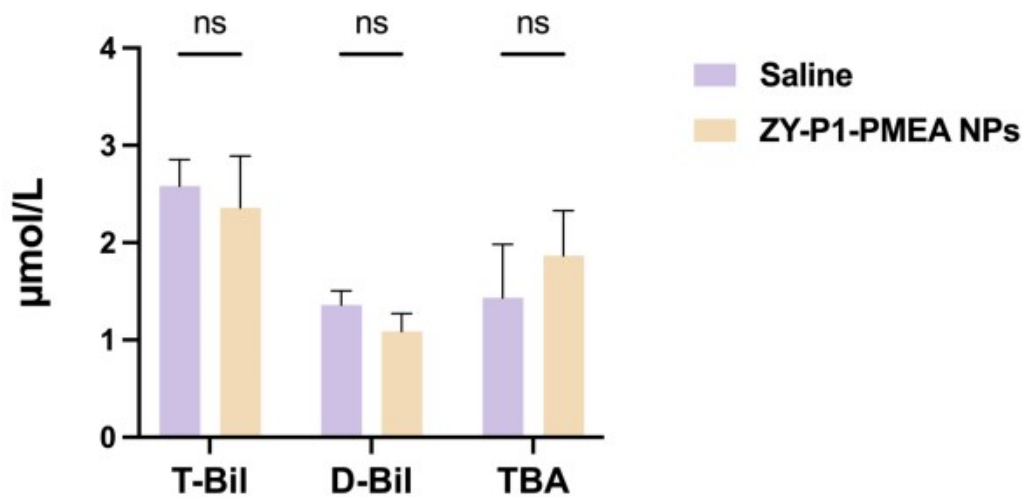


Figure S45. Quantitative analysis of T-Bil, D-Bil and TBA of *AopE*^{-/-} mice following treatment with saline and **ZY-P1-PMEA** NPs. T-Bil = Total Bilirubin, D-Bil = Direct Bilirubin, TBA = Total Bile Acids.

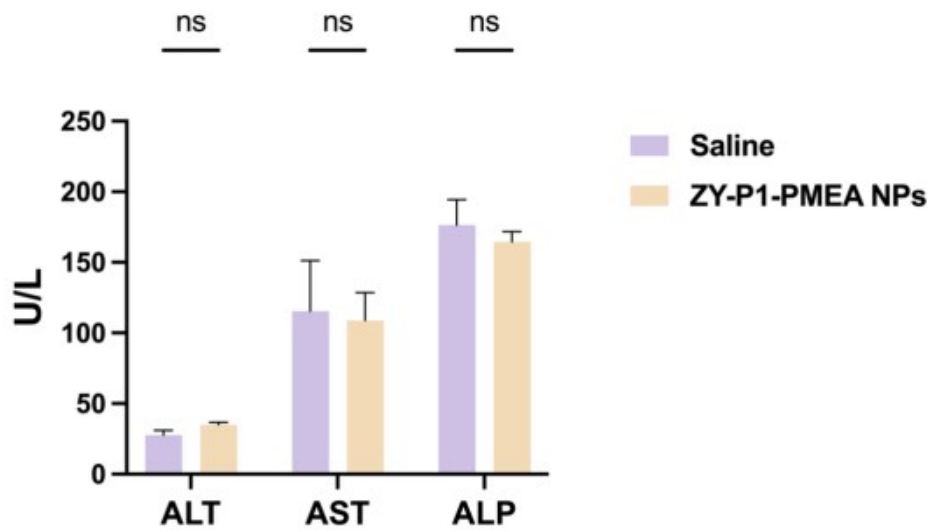


Figure S46. Quantitative analysis of ALT, AST and ALP of *AopE*^{-/-} mice following treatment with saline and **ZY-P1-PMEA** NPs. ALT = Alanine Aminotransferase, AST = Aspartate Aminotransferase, ALP = Alkaline Phosphatase.

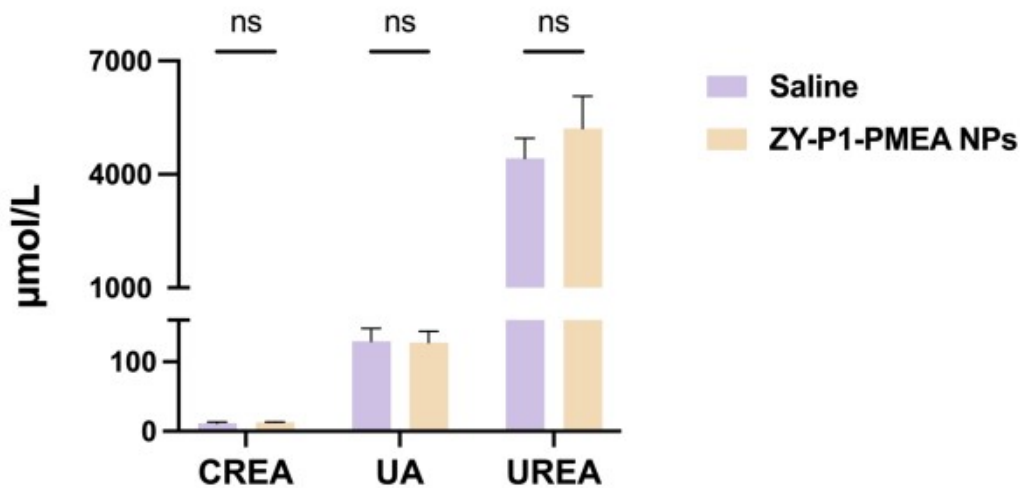


Figure S47. Quantitative analysis of CREA and UREA of *AopE*^{-/-} mice following treatment with saline and **ZY-P1-PMEA** NPs. CREA = Creatinine, UA = Uric Acid, UREA = Urea.